ASSESSING THE FEASIBILITY AND ECONOMIC VIABILITY OF SOLAR CPC FOR ABSORPTION COOLING SYSTEM IN DIVERSE INDIAN CLIMATE ZONES

Aditi Garg, Bahni Ray and Sanjeev Jain

Department of Mechanical Engineering, Indian Institute of Technology Delhi, New Delhi (India)

Abstract

The present work analyzes the feasibility of a solar absorption cooling system in the Indian context. A compound parabolic collector (CPC) is used with a single-effect vapour absorption chiller to meet a building cooling load. The thermal economic and environmental performance analysis is carried out for four cities in different climate zones of the country using TRNSYS software. The effect of parameters like solar collector area, storage volume, and collector slope have been observed on the solar fraction (SF), auxiliary heat energy consumption, collector useful energy gain, payback period (PBP), and levelized cost of cooling (LCOC). The optimized values of the parameters have been decided based on the payback period and solar fraction.

Keywords: TRNSYS, Solar cooling, CPC, economic analysis, absorption chiller

1. Introduction

India, geographically positioned between 8°4' north to 37°6' north, boasts a wide range of climates, encompassing hot and dry, warm and humid, moderate, cold, and composite regions. As the country experiences rising temperatures, the demand for space cooling is set to surge, further burdening the power grid. While India has made substantial progress in harnessing renewable resources, there remains untapped potential for further exploration. Solar energy, in particular, has gained considerable momentum in various applications, including solar cooling. Solar cooling is one of the most promising technologies as it may lead to a decrease in electricity consumption in summer and has great compatibility between source supply and load demand.

Among the various options available for solar cooling technologies, the vapor absorption cooling system stands out as a popular option, primarily because of its high efficiency and the successful commercialization of absorption chillers (Xu and Wang, 2017). Absorption chillers demonstrate superior coefficient of performance (COP) values compared to other solar cooling technologies, typically ranging from 0.6 to 0.8 for single-stage chillers and from 0.9 to 1.3 for two-stage chillers. Two common solution pairs used as refrigerant-sorbent in absorption chillers are ammonia-water and water-lithium bromide. Ammonia-water systems can achieve evaporator temperatures below 0 °C, while water-lithium bromide systems can reach temperatures as low as 4 °C.

The operating temperature for single-stage absorption systems can be provided by solar collectors such as flat plate collectors (FPC), evacuated tube collectors (ETC), and compound parabolic collectors (CPC). Among them, CPC can provide a low concentration in the range of 2-10 and operate in the medium temperature range of 100 ºC -120 ºC. It provides an advantage over non-concentrating collectors like flat plate collectors (FPC) and evacuated tube collectors (ETC) by providing concentration and an advantage over concentrating collectors like a parabolic trough and parabolic dish by their ability to collect both direct and diffuse radiations without employing tracking system. Due to this, it has gained worldwide attention in the last few decades for its use in multiple applications, including solar absorption cooling.

A lot of research has been done on solar absorption cooling integrated with different types of collectors throughout the world. Various companies have installed solar cooling setups in various institutions for space-cooling applications. There are various factors that influence the technical feasibility of these systems, such as the availability of required solar radiation, cost of components, electricity and fuel costs, water, and land availability. Apart from the technical feasibility of the solar cooling system, it must be economically attractive for the developers and investors to fund the system. The useful lifetime period of these systems is 20 years to 25 years. The government also occasionally launches various policies and subsidies to encourage the development of these non-conventional energy systems and reduce the load on the power grid. Environmental assessment is also carried out to determine how much carbon footprint reduction occurs by employing these technologies. Many experimental and simulation studies have been carried out to investigate and improve the performance of solar vapour absorption cooling systems. The simulation studies have mostly been carried out using Transient System Simulation (TRNSYS) software for modelling and simulating the absorption cooling system with different solar collectors. Many studies have analysed the effects of solar collector area, storage tank volume, boiler set point, collector mass flow rate, and solar collector

10.18086/swc.2023.04.05 Available at http://proceedings.ises.org

slope on the thermal, economic, and environmental performance of the solar cooling system and have suggested optimized values of the parameters.

Florides et al. (2002) explored the performance of different types of solar collectors, such as FPC, CPC, and ETC, for an absorption cooling system for residential cooling in Nicosia, Cyprus, using TRNSYS. Assilzadeh et al. (2005) modeled and simulated a single-effect LiBr-water absorption system with ETC for Kuala Lumpur, Malaysia. Hang et al. (2011) analyzed the performance of ETC based absorption cooling system for Los Angeles, California, and concluded that the cost of carbon footprint reduction is the key indicator for the sizing and overall performance of the system. Al-Alili et al. (2012) studied the feasibility of ETC based ammonia water-driven solar cooling system for Abu Dhabi. They suggested a specific collector area and specific tank size with regard to chiller capacity and compared the electrical consumption with vapor compression cooling systems. Xu and Wang (2017) carried out the analysis of CPC-based absorption cooling systems with single-effect, double-effect, and variable-effect absorption chillers for Miami. The performance of variable effect was found to be better, followed by single-effect and double-effect chillers. Sokhansefat et al. (2017) modelled and simulated an existing ETC-based absorption cooling system installed in Tehran, Iraq. A parametric analysis was conducted, and optimized parameters were obtained, which resulted in the enhancement of solar fraction by 28%. Bellos and Tzivanidis (2017) conducted simulation studies for ETC-based absorption cooling systems for ten locations worldwide. Different sets of collector area and storage tank volumes were investigated in order to obtain optimised values for achieving minimised levelized cost of cooling.

Khan et al. (2018) developed and analysed two configurations for solar vapour absorption systems for FPC and ETC for Islamabad in Pakistan. The system performance of two configurations, along with the two collectors, were compared for solar fraction, collector efficiency, and primary energy savings for different collector slopes, collector areas, and storage tank volumes. Altun and Kilic (2020) modelled and analysed an absorption cooling system for FPC and ETC for six cities located in Turkey for various parameters, and solar fraction, levelized cost of cooling, and payback period were plotted for optimum values of parameters.

In the Indian context, few studies have also been conducted to study the potential of solar absorption cooling in some cities. Uttham et al. (2016) analysed the performance of an absorption cooling system with ETC for an office building in Gandhinagar, Gujarat, India. The study also explored optimising parameters such as storage tank volume, collector area, and collector slope. Muye et al. (2016) investigated the performance of ammonia–water absorption power and cooling systems with CPC and biomass auxiliary heater for Chennai (India) and Seville (Spain). The scroll expander was utilised for power generation. The study concluded that increasing the absorber temperature is advantageous for power production while raising the evaporator temperature is detrimental to cold production. Additionally, elevating the condenser temperature is unfavourable for both outputs, with Seville demonstrating better system performance but Chennai achieving a higher solar fraction. Narayanan (2017) conducted a techno-economic analysis for an absorption cooling system with ETC for an office building in Chennai. It was found that the proposed solar absorption cooling system would achieve a full payback after 15.5 years, in contrast to a traditional air conditioner unit. Further, it was noted that this payback period could vary depending on the local climate and cooling demand. Gogoi and Saikia (2019) analysed the performance of a combined solar-powered organic Rankine cycle and absorption cooling system using a parabolic trough collector (PTC) for four months in Jodhpur, India. Five different working fluids were compared for the Rankine cycle. The absorption cooling system performance was compared at two generator temperatures. Sharma et al. (2023) conducted thermal and economic analysis for a solar absorption cooling system using CPC for milk chilling application for an experimental prototype in Jaipur, India. The levelized cost of energy, simple payback period, and discounted payback period were estimated as 0.177 $/kWh, 12.4 years, and 19.7 years.

Despite the growing market presence of solar cooling installations by various Indian companies, there is a notable lack of comprehensive research in this domain, particularly regarding the Indian context. Given that cooling requirements often outweigh heating loads in the Indian climate, solar cooling technologies are of paramount importance. This study aims to bridge this research gap by investigating the feasibility of utilizing CPC-based solar absorption cooling in four major Indian cities: New Delhi, Chennai, Bengaluru, and Ahmedabad. These cities are strategically chosen to represent diverse climate zones within the country. This analysis not only focuses on assessing the thermal performance of the system but also examines the economic viability and environmental analysis of implementing solar cooling systems in these regions.

2. Methodology Overview

2.1 Description of solar cooling system configuration

A solar cooling system has been made in TRNSYS to meet a design cooling load of 100 kW, as shown in Fig. 1. The picture of the solar cooling system for the analysis is shown in Fig.2. Compound parabolic collectors (CPC) have been used with a single-effect vapour absorption chiller to meet the cooling demand using solar energy. The hot water generated by the solar collector is stored in the storage tank and used to power the absorption chiller. An auxiliary boiler is placed between the storage tank and the absorption chiller to ensure the water temperature stays at the desired level. This heater is used when the water temperature falls below the desired temperature. The absorption chiller generates chilled water, which is utilized to meet the building cooling requirements. TMY data is obtained from the Meteonorm database of the TRNSYS library. The system is run in the summer season in India, typically from 1st April to 30th September, for 12 working hours. The same cooling load has been analyzed for all cities to compare the system's feasibility for the location. The building hourly cooling load has been generated using a building load generator component in TRNSYS. The details of the single-effect vapour absorption chiller are mentioned in Table 1. A chiller with a capacity of 125 kW is found to be suitable to meet the peak load. The set point of hot water temperature is considered to be 115 ºC. The flow rates for hot, chilled, and cooling water are calculated as per the details mentioned in TRNSYS documentation.

Table 1 Chiller Specifications

Parameter	Value	Units
Rated chiller capacity	125	kW
Rated chiller COP	0.7	-
Chilled water temperature (inlet/outlet)	12.22/6.67	°C
Chilled water flow rate	4.297	kg/s
Hot water temperature (inlet/outlet)	115/105	°C
Hot water flow rate	3.4094	kg/s
Cooling water temperature (inlet/outlet)	29.44/32.22	°C
Cooling water flow rate	21.02	kg/s
Electrical power	2	kW

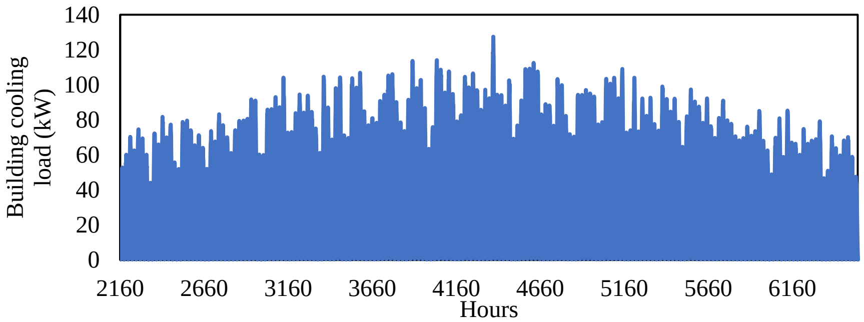

Fig. 1 Building cooling load for the period from 1st April to 30th Sep (2160 to 6552 hours)

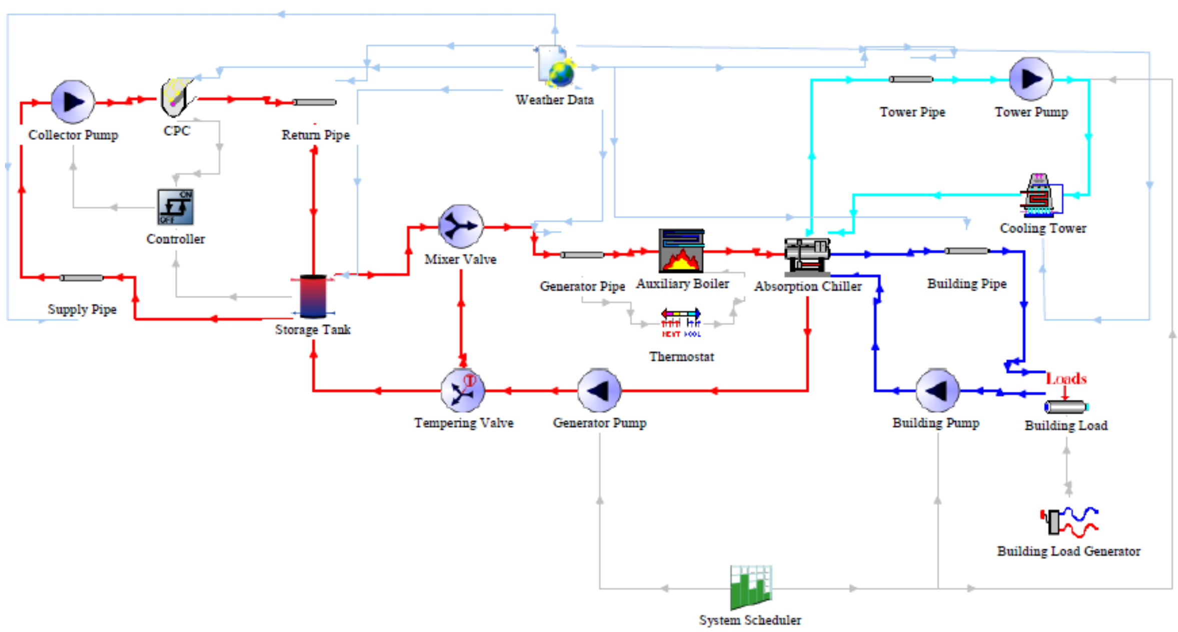

Fig. 2 Solar absorption cooling system model in TRNSYS

2.2 Modelling of system in TRNSYS

The solar absorption cooling system has been modelled in TRNSYS software (v18). The system can be divided into two subsystems: solar collector system and absorption cooling system. The solar collector system includes solar collectors, storage tank, controllers, and collector pumps. The absorption cooling system includes an absorption chiller, pumps, auxiliary heater, controllers, valves, cooling tower, and building cooling load. The various components used are discussed in the subsequent sections. Fig. 2 shows the picture of the solar cooling system modelled in TRNSYS. The model of the system has been developed considering the following assumptions taken from the literature:

- Heat losses are only considered within the storage tank, with no consideration for heat losses in the pipelines and valves.
- Flow mixing within the storage tank is assumed to be adiabatic and perfectly mixed.
- Thermal properties of water are assumed to remain constant throughout the analysis.
- Potential effects of water boiling or freezing within the solar loop are not factored into the calculations.
- Thermal storage tank is oriented vertically to promote thermal stratification.

2.2.1 Weather Data

The weather data has been obtained using the component Type 15-6, which uses a typical meteorological year 2 (TMY-2) data file. This data file provides the solar radiation, dry bulb temperature, and other weather conditions for New Delhi, India. The diffuse solar radiation on the tilted surface has been calculated using the Perez model. This component also takes the values of the slope and azimuth angle for the collector considered. The weather data is taken from 1st April to 30th September (2160h to 6552h), and the simulation time step is taken as 5 minutes.

2.2.2 Solar Collector

The collector was designed using the compound parabolic collector (CPC) model found in the TRNSYS library (TYPE 74). This particular TYPE necessitates multiple inputs for an efficient collector model, including collector area, fluid-specific heat, overall heat loss coefficient, orientation, optical and geometrical parameters. Table 2 contains detailed information on the collector's specifications.

Table 2 Specifications of solar collector

Parameter	Value	Units
Fluid specific heat	4.19	kJ/kg.K
Collector fin efficiency factor	0.85	-
Overall heat loss coefficient	0.833	W/m^2.K
Wall reflectivity	0.9	-
Half-acceptance angle	30	º
Truncation ratio	0.7	-
Axis orientation	1	-
Absorptance of absorber plate	0.85	-
Number of covers	1	-
Index of refraction of cover	1.526	-
Extinction coeff. thickness product	0.0026	-

2.2.2 Storage tank

The storage tank has been modelled using the component TYPE 4a. It is segmented into ten equal-volume segments, each fully mixed, to introduce thermal stratification. The inlets and outlets of the tank are at a fixed position. The hot fluid flows into the tank's upper portion, while the cold fluid enters from the lower section.

2.2.3 Auxiliary heater

A steam boiler is used to provide auxiliary heating for the system and is modelled using Type 700. In this model, the boiler efficiency and the combustion efficiency are supplied as inputs to the model. This component (Type700) assumes that device efficiency is not a function of inlet conditions. It is connected to a thermostat (Type 108), which checks the incoming fluid temperature, and if it is less than the chiller hot water set point temperature, it turns on the auxiliary heater else it remains switched off.

2.2.4 Absorption Chiller

The vapour absorption chiller has been modelled using Type 107. It considers a single effect hot water driven LiBr-H_2O based water-cooled vapour absorption chiller. An external file is utilized to provide performance data for this absorption chiller. This external file contains data points representing the fraction of nominal capacity and the fraction of design energy input for various sets of fractions of design energy load, chilled water setpoint temperature, inlet cooling water temperature, and inlet hot water temperature. This data file is available in the software database. The chiller's specifications can be found in Table 1. Additionally, the electrical power required to operate the chiller's pumps is determined based on information sourced from THERMAX company's absorption chiller brochures.

2.2.5 Cooling Tower

A closed-circuit cooling tower has been modelled using the component Type 510. It provides cooling water to remove heat from the absorber and condenser of the absorption chiller. This cooling tower cools a liquid stream by evaporating water from the outside of coils containing the working fluid. The working fluid is completely isolated from the air and water in this type of system.

2.2.6 Other components

The fluid flow rates in the various loops in the system are operated using single-speed pumps (Type 114). The pump in the collector circuit is operated by the control signals of the differential controller (Type 2b). This controller switches on the pump when the collector outlet temperature exceeds the outlet temperature at the bottom of the storage tank by 3 ºC and switches off if this difference is less than 0.5 ºC (Al-Alili et al., 2012). Pipes are modelled by Type 31 and are sized with at least enough volume to handle the flow during one timestep. The tempering valve (type 11b) compares the temperature of the hot water returning from the chiller with the outlet temperature of the hot water at the top of the tank. If the returning hot water temperature exceeds the tank outlet temperature, the valve bypasses the full flow directly toward the auxiliary heater; otherwise, it is sent to the storage tank. The flow mixer (Type 11h) only facilitates the flow either from the tempering valve or the storage tank. The system's operational schedule is managed by a forcing function component (Type 14h) and is considered for 12 hours daily, from 7 am to 7 pm. Finally, the results are obtained using a plotter (Type 65d) and a printegrator (Type 46a).

2.2.7 Building load

The building load profile for the given system is generated using a synthetic building load generator component (Type 686) in TRNSYS. This component generates hourly cooling loads by employing user-defined parameters for peak cooling design load. It incorporates sinusoidal functions that adjust for seasonal fluctuations, time-of-day variations, and differences between weekdays and weekends. This modeling approach rapidly generates realistic loads, circumventing the labour-intensive process of modeling a real building.

For this study, we consider a peak cooling design load of 100 kW for the building. The actual load may exceed this value due to factors such as noise, multiplier, and offset parameters.

The generated building load profile is characterized as the cooling load for component Type 682. This component essentially imposes the load on the chilled water flowing through it and computes the resulting conditions of the outlet chilled water. Conceptually, it serves as an interface between the building load and the working fluid within an HVAC system.

2.3 Thermal analysis of solar cooling system

The thermal performance of the solar cooling system is evaluated using solar fraction (SF), which is defined as the amount of useful energy gain by the solar collector (E_u) to the total energy required for water heating for the absorption chiller, which includes both useful energy gain by collector (E_u) and auxiliary heat provided by the boiler (E_{aux}) as mentioned in eq. 1. The design parameters such as solar collector area, storage tank volume, and collector slope are varied to study their effect on solar fraction.

$$SF = \frac{E_u}{E_u + E_{aux}} \qquad \text{(eq. 1)}$$

2.4 Economical analysis of solar cooling system

The value of any energy system must ultimately be judged based on its economy. The total cost of the system includes capital cost, installation cost, maintenance, and operating costs. The capital and installation costs are one-time costs that need to be paid once in the useful lifetime of the solar cooling system. In contrast, maintenance and operating costs are periodical costs that must be paid annually. Capital Cost (C.C) is the total cost of all the components used in the system. The installation cost (I.C) is the cost incurred in installing and integrating the system, assuming 25 % system installation and 20 % system integration cost of the capital cost (Eicker and Pietruschka, 2009). The sum of capital cost and installation cost is the total initial investment cost (C_o) required to set up the solar cooling system. The capital cost and installation cost (C.C and I.C) must be converted to equivalent annualised investment cost (C_{o_annual}) as they are a one-time cost and must be added to yearly operation and maintenance costs. The expressions for all the costs are given from eq. (2)-(5). The details of economic parameters are specified in Table 3.

$$C.C = C_{SC}A_{SC} + C_{ST}V_{ST} + C_{ABS}Q_{ABS} + C_{CT}Q_{CT} \quad \text{(eq. 2)}$$

$$I.C = 0.45\ C.C \quad \text{(eq. 3)}$$

$$C_O = C.C + I.C \quad \text{(eq.4)}$$

$$C_{o\_annual} = C_O\left(\frac{d(1+d)^N}{(1+d)^N - 1}\right) \quad \text{(eq.5)}$$

Table 3 Components costs

Components	Value	Unit	Ref.
Solar collector cost (C_{SC})	12000	INR/m^2	Pranesh et al. (2019)
Storage tank (C_{ST})	60000	INR/m^3	Sharma et al. (2023)
Absorption chiller (C_{ABS})	60000	INR/TR	Utham et al (2016)
Cooling tower (C_{ST})	1400	INR/ TR	Sharma et al. (2023)
Market discount rate (d)	6	%	Sharma et al. (2023)
Investment lifetime (N)	25	Years	Sharma et al. (2023)
Fuel inflation rate (FIR)	5	%	Jha et al. (2022)
Fuel cost (C_{FUEL})	5.010	INR/ kWh	Global Petrol Prices (2023)
Electricity cost (C_{ELE})	10.08 (New Delhi)	INR/ kWh	Gill et al. (2017)

Maintenance Cost ($M.C_{annual}$) is the cost incurred in maintaining and repairing the system, and it is considered to be 2% of the total initial investment cost (Co) (Eicker and Pietruschka, 2009, Hang et al., 2012). The operating cost ($O.C_{annual}$) is the cost incurred in total electric power consumption of the system and natural gas consumption by the auxiliary heater (Hang and Ming, 2012). The operating cost for the first year ($O.C_{first\ year}$) is the sum of the total fuel consumption cost in the auxiliary heater and the electricity consumption cost of the total system. Finally, the total annualised cost (T.A.C) is calculated as the sum of all annualised equivalent costs. The expressions for the costs are given from Eq. (6)-(8).

$$M.C_{annual} = 0.02C_o \quad \text{(eq.6)}$$

$$O.C_{annual} = O.C_{first\ year}\left(\frac{1-\left(\frac{1+FIR}{1+d}\right)^N}{(d-FIR)}\right)\left(\frac{d(1+d)^N}{(1+d)^N-1}\right) \quad \text{(eq.7)}$$

$$T.A.C = C_{o\_annual} + M.C_{annual} + O.C_{annual} \quad \text{(eq.8)}$$

The payback period (PBP) and the levelized cost of cooling (LCOC) are two economic indicators that analyses the economic performance of the system. The payback period is defined as the time needed for cumulative fuel savings to be equal to the total initial investment in the system. It must be less than the useful lifetime of the system (N) for the system to be economically viable. PBP is of two types: Simple PBP and Discounted PBP. Simple PBP considers only the market discount rate, while discounted PBP considers the time value of money by incorporating both the market discount rate and inflation rate and is more realistic. Levelized cost of cooling (LCOC) is the unit cost of cooling provided by the cooling system. The expressions for the economic indicators are given from Eq. (9)-(11).

$$\text{Simple PBP} = \frac{\ln\left(1+\frac{C_o.d}{E_U C_{Fuel}}\right)}{\ln(1+d)} \quad \text{(eq.9)}$$

$$\text{Discounted PBP} = \frac{\ln\left(1+\frac{C_o.(FIR-d)}{E_u C_{Fuel_{first\ year}}}\right)}{\ln\left(\frac{1+FIR}{1+d}\right)} \quad \text{(eq.10)}$$

$$LCOC = \frac{\text{Total annual cost (TAC)}}{\text{Total cooling energy generated annually (Ecool)}} \quad \text{(eq.11)}$$

2.5 Environmental analysis of solar cooling system

The environmental analysis of the solar cooling system is based on the amount of carbon dioxide emission avoided by using VAS instead of VCS. The carbon dioxide emitted (CDE_{VAS}) during the operating phase of the VAS solar cooling system is calculated as the sum of emissions due to natural gas combustion in the auxiliary heater (CD_{ENG}) and emissions due to the electrical consumption by the chiller (CDE_{ELE}) as given by eq. (12). The carbon dioxide emission factor for electricity (EF_{ELE}) is considered as 0.81 kg/ kWh (Bhawan and Puram, 2022), and the carbon dioxide emission factor for natural gas is taken as (EF_{NG}) is considered as 0.2 kg/ kWh (Balghouthi et al., 2012). The electrical energy consumption (E_{ELE_VAS}) and thermal energy provided by natural gas (E_{NG}) are multiplied by their respective emission factors (EF), as shown in eq.(13)-(14). An electrical chiller (or VCS) of equivalent capacity for COP of 2.4 for the same building cooling load and ambient conditions is considered, and carbon dioxide emission due to electrical consumption by this chiller (CDE_{VCS}) is calculated by eq. (15). The difference between the carbon dioxide emissions of VAS and VCS is amount of carbon dioxide emissions avoided ($CDE_{avoided}$) given by eq. (16).

$$\mathrm{CDE_{VAS}} = \mathrm{CDE_{ELE}} + \mathrm{CDE_{NG}} \quad \text{(eq. 12)}$$

$$\mathrm{CDE_{ELE}} = \mathrm{E_{ELE\_VAS}} \times \mathrm{EF_{ELE}} \quad \text{(eq. 13)}$$

$$\mathrm{CDE_{NG}} = \mathrm{E_{NG}} \times \mathrm{EF_{NG}} \quad \text{(eq. 14)}$$

$$\mathrm{CDE_{VCS}} = \mathrm{E_{ELE_{VCS}}} \times \mathrm{EF_{ELE}} \quad \text{(eq. 15)}$$

$$\mathrm{CDE_{avoided}} = \mathrm{CDE_{VCS}} - \mathrm{CDE_{VAS}} \quad \text{(eq. 16)}$$

3. Results and Discussion

This section presents the results of the parametric analysis for the modelled solar cooling system. The simulations were carried out with a time step of 5 min from 1st April to 30th Sep (2160h to 6552h). The parameters considered for the analysis are solar collector area, collector slope, and storage tank volume. The solar collector area varies from 100 m^2 to 1000 m^2 with a step size of 100 m^2, collector slope from 0° to 30° with a 5° step size, and storage tank specific volume ratio from 0.02 m^3/m^2 to 0.1 m^3/m^2 with a step size of 0.02 m^3/m^2. Four cities have been chosen to represent four different climate zones of the country, as tabulated in Table 4. It can be noted that the four cities have similar values of incident horizontal solar radiation received but have different climatic zones.

Table 4 List of cities considered

Climate zone	Cities	Total horizontal solar radiation (kWh/m^2)
Hot & dry	Ahmedabad	1077.37
Warm & humid	Chennai	1073.71
Moderate	Bengaluru	1023.23
Composite	New Delhi	1118.79

3.1 Collector area

The solar collector area is an important parameter for optimizing the solar cooling system. The solar collector area is varied from 100 m^2 to 1000 m^2 with a step size of 100 m^2. Fig. 3 shows the variation of collector useful energy gain, auxiliary heat energy consumption, and solar fraction with collector area, keeping collector slope and storage tank volume fixed. It is observed that collector useful energy gain and solar fraction increase with collector area while the auxiliary heat energy consumption decreases. The increment in solar fraction decreases with the collector area and eventually leads to the fact that after a certain value of collector area, solar fraction will become constant. It is noted that after a collector area of 400 m^2, the auxiliary energy starts becoming lesser than the useful energy gain, indicating that at least a minimum of 400 m^2 is required to meet the cooling load. The solar fraction becomes 47% at an area of 400 m^2. So, the system must have enough capacity to provide at least half of the required heat through the solar collector system. Fig. 4 shows the effect of the collector area on LCOC and PBP.

LCOC initially decreases with the collector area and then starts increasing, while PBP is found to decrease with the collector area. The change in PBP decreases as the collector area increases, so greater areas have no significant economic advantage. Also, the discounted PBP is higher than the simple payback period as it incorporates the time value of money. The discounted PBP becomes economically feasible after the collector area greater than 400 m^2 for the PBP is 23 years. Fig.5 shows the variation of carbon dioxide emissions (CDE) of the vapour absorption system (VAS) with collector area and compares it with a conventional vapour compression system (VCS) and also shows how much CDE is avoided if VAS replaces the VCS system. The CDE of VAS decreases with the collector as the amount of auxiliary energy required decreases with the collector area. However, the change in CDE avoided decreases as the collector area increases because of the slow increase of solar fraction.

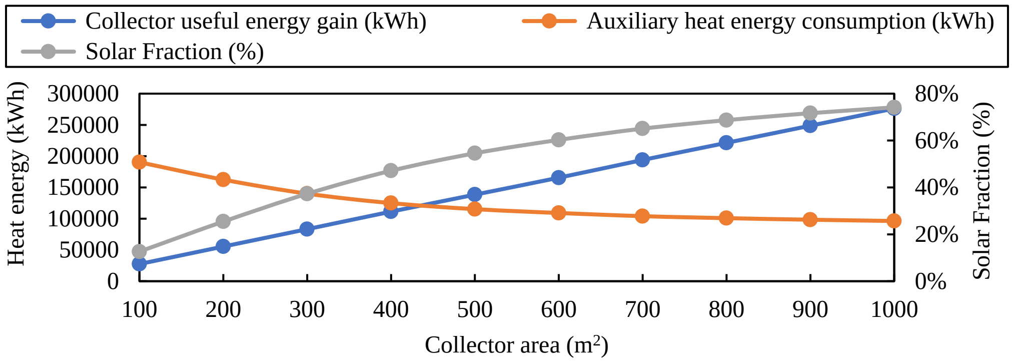

Fig. 3 Variation of collector useful energy gain, auxiliary heat energy consumption, and solar fraction with collector area

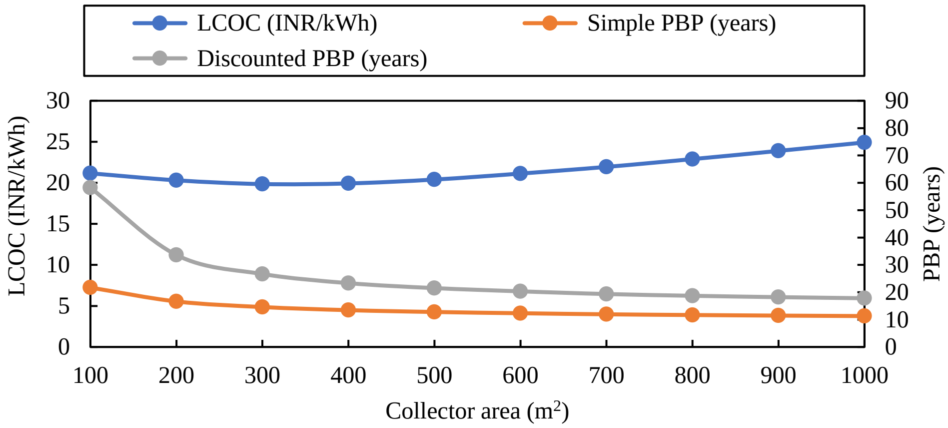

Fig.4 Variation of LCOC, simple and discounted PBP with collector area

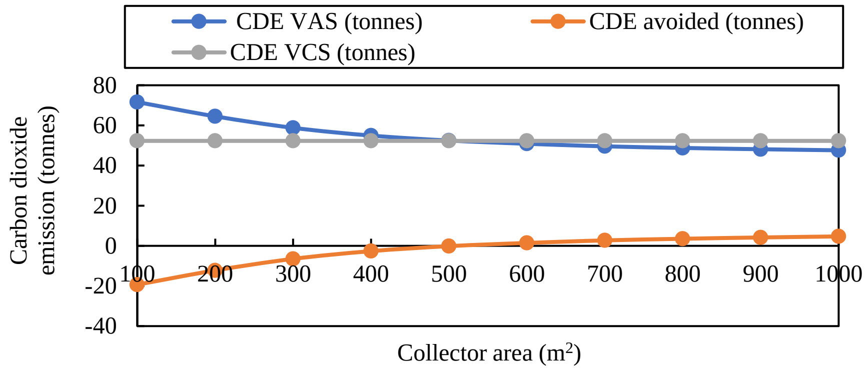

Fig.5 Variation of carbon dioxide emissions with collector area

3.2 Collector slope

Fig.6 shows the variation of collector useful energy gain, auxiliary heat energy consumption, and solar fraction with collector slope, keeping collector area and storage tank volume fixed. The collectors are assumed to be south-facing by keeping their azimuth angle 0º. The solar fraction and collector useful energy gain increases and becomes maximum at 10º, then decreases with the collector slope. The auxiliary heat energy consumption decreases, becomes minimum, and then increases. The solar fraction at the collector slope of 10º is more than 6% than at the location's latitude (28º). Fig. 7 shows the effect of the collector slope on LCOC and PBP, and it can be observed that the collector slope has an insignificant influence on these economic parameters, and they achieve minimum values at 10º as well. The CDE does not change much with the slope and increases after the slope is greater than 20º (Fig.8). This indicates that the collector slope can be optimised based on the thermal analysis as it does not have a considerable impact on economic and environmental analysis.

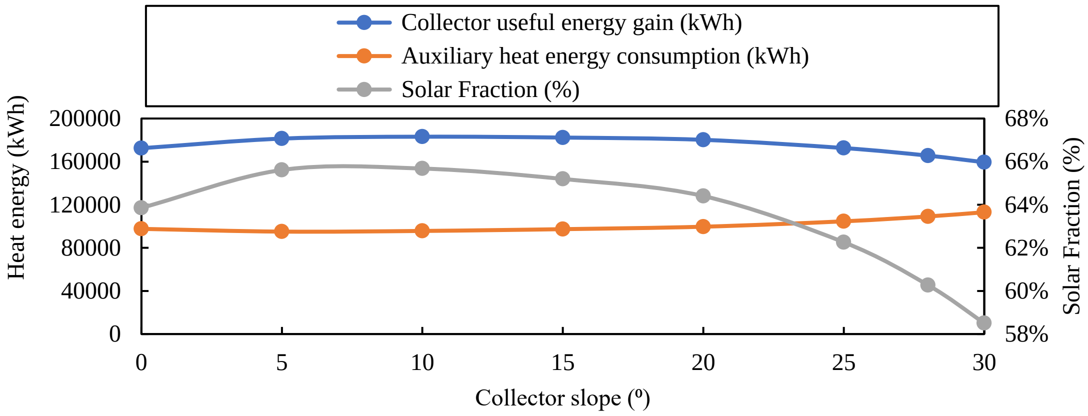

Fig. 6 Variation of collector useful energy gain, auxiliary heat energy consumption, and solar fraction with collector slope

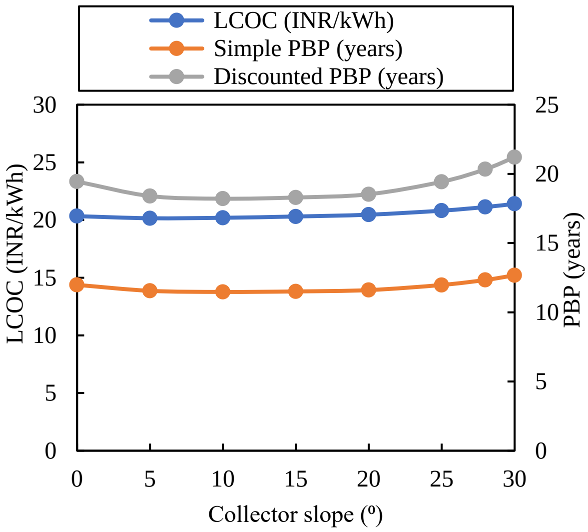

Fig. 7 Variation of LCOC, simple and discounted PBP with collector slope

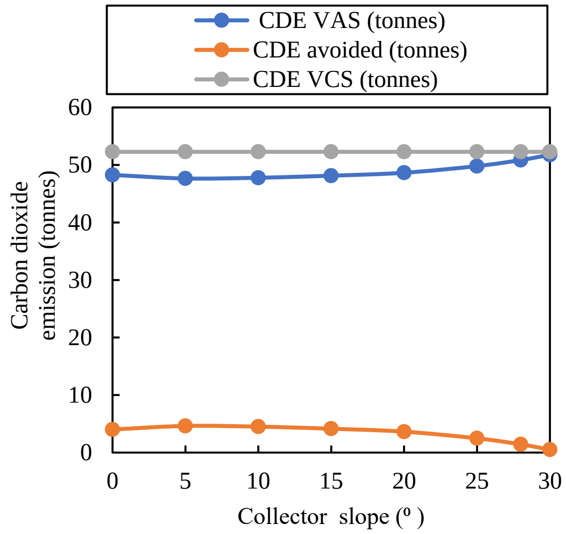

Fig. 8 Variation of carbon dioxide emissions (CDE) with collector slope

3.3 Storage tank specific volume ratio (STSVR)

The storage tank specific volume ratio (STSVR) is varied from 0.02 to 0.1 m^3/m^2 of solar collector area for a step size of 0.02 m^3/m^2 (Hang et al., 2011). Fig. 9 shows the variation of solar fraction with storage tank specific volume ratio (STSVR) for different collector areas. The solar fraction decreases with STSVR for a given collector area, indicating that storage tank volume does not significantly affect the system's thermal performance for small collector areas. The solar fraction increases with collector area as there is a proportional increase in storage tank volume. A few runs for STSVR of 0.01 and collector areas of 1100 m^2 and 1200 m^2 were also done. It was observed that for an area greater than 1000 sq.m, solar fraction increases from the ratio of 0.01 to 0.02 and then decreases. For all areas, the change in solar fraction is less when the ratio varies from 0.01 to 0.02 than the other ratios. There seems to be no advantage when the ratio is more than 0.02

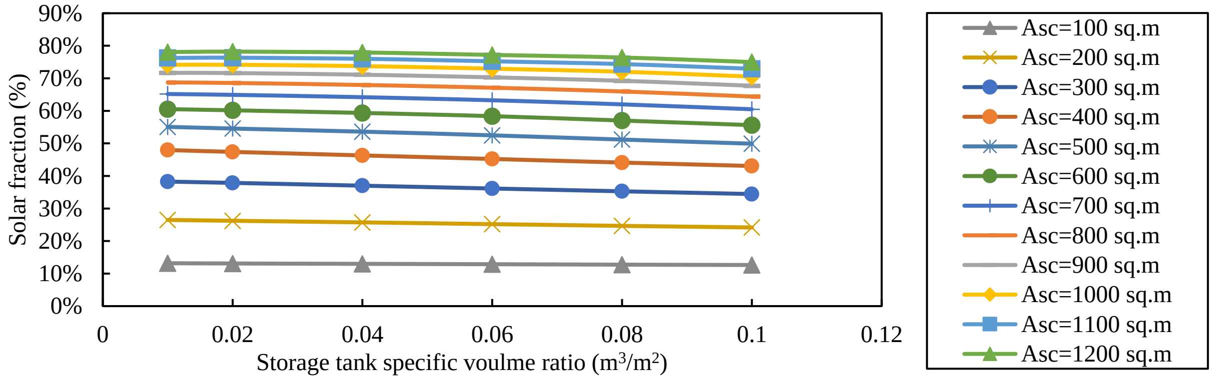

Fig. 9 Variation of solar fraction with storage tank specific volume ratios (STSVR) for different collector areas.

Fig. 10 and Fig. 11 show the effect of storage tank-specific volume ratio on LCOC and PBP. These economic parameters increase with STSVR as the collector area and storage tank volume contribute majorly to the initial investment cost. In Fig.11, many ratios give PBP greater than 25 years, which makes them economically unfeasible. The carbon dioxide emissions by the absorption system are shown in Fig. 12, increasing with the ratio for a given area due to an increase in auxiliary heat energy consumption.

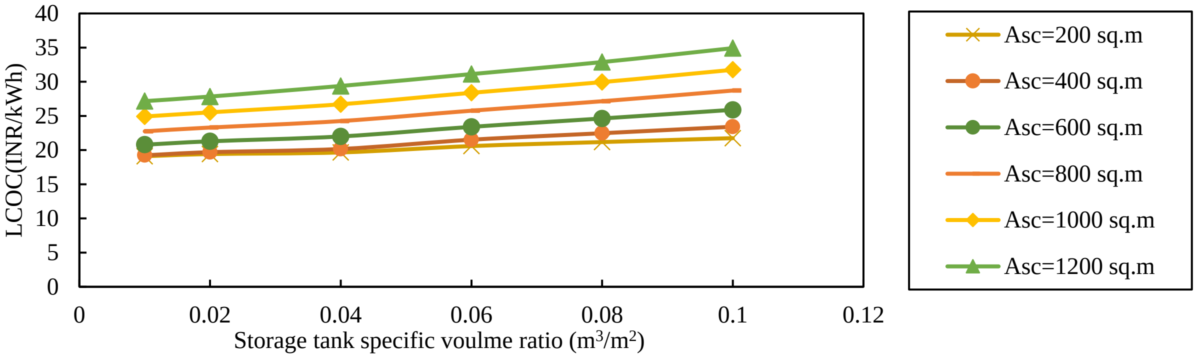

Fig. 10 Variation of LCOC with storage tank specific volume ratios (STSVR) for different collector areas

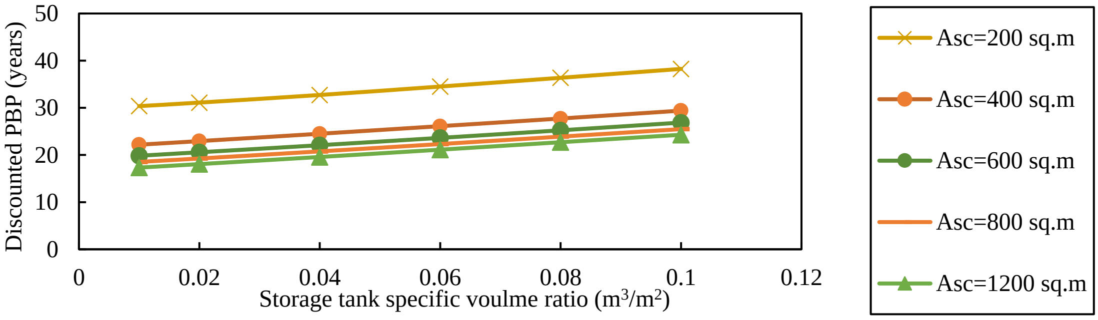

Fig. 11 Variation of PBP with storage tank specific volume ratios (STSVR) for different collector areas

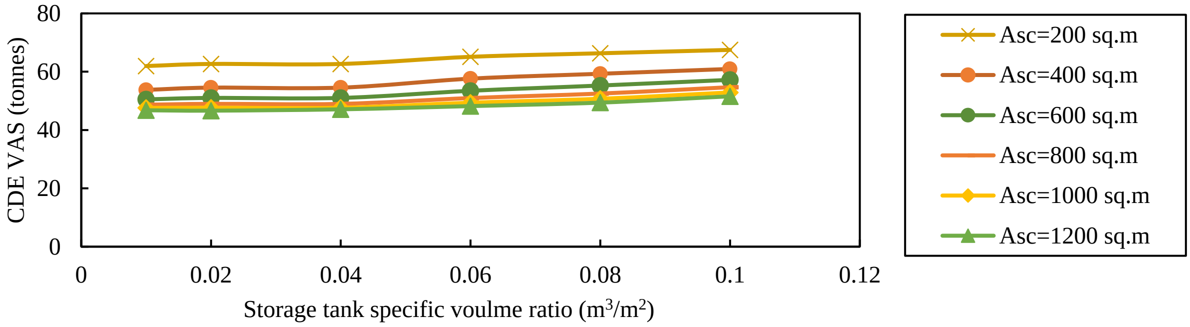

Fig. 12 Variation of CDE associated with solar vapour absorption system with storage tank specific volume ratios (STSVR) for different collector areas.

3.4 Optimisation of parameters

The collector area has a major impact on thermal, economic, and environmental analysis, while the effect of the collector slope is limited to thermal analysis. The storage tank-specific volume ratio does not significantly affect the thermal analysis, and increasing it has no economic advantage for a given collector area. So, from the preceding section, the optimum storage tank-specific volume ratio is considered 0.02 for further analysis. The collector slope is optimised based on a maximum solar fraction, as shown in Fig. 13, for a fixed collector area.

Fig.14 shows the variation of the payback period with the collector area for the four cities considered for the optimised collector slope. The payback period decreases with the collector area; after a particular value, the change in PBP is insignificant to the increase in the collector area. So, that value for the collector area is considered an optimized area. The list of optimized parameters has been tabulated in Table 5.

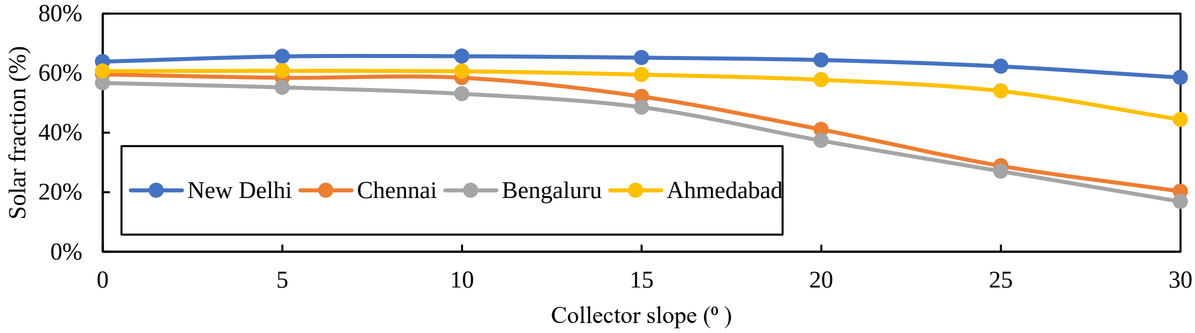

Fig. 13 Variation of solar fraction with collector slope for different cities for a fixed collector area and storage tank specific volume ratio

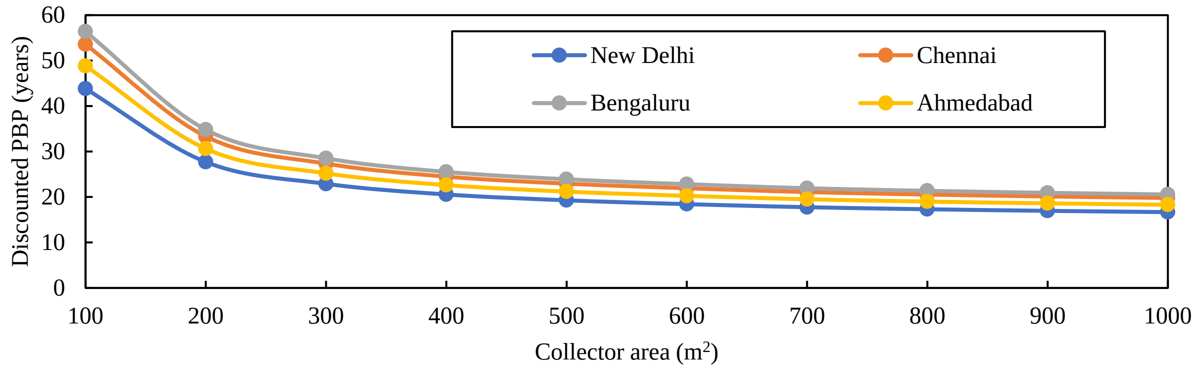

Fig. 14 Variation of PBP with collector area for different cities for optimised collector slope and storage tank specific volume ratio

Table 5 List of optimized results for four cities

Cities	Total horizontal solar radiation (kWh/m²)	Electricity tariff (INR/kWh)	Collector area (m²)	Storage volume (m³)	Collector slope (°)	TAC (INR)	SF (%)	Discounted PBP (years)	LCOC (INR/kWh)	CDE VAS (tonnes)
Ahmedabad	1077.3	6.47	600	12	5	2900938	60.8	20.25	20.06	50.92
Bengaluru	1023.2	6.62	700	14	0	3120266	61.4	21.93	21.58	51.35
Chennai	1073.7	10.29	700	14	0	3185328	64.5	21.09	22.03	48.91
New Delhi	1118.7	10.08	600	12	10	2945037	65.5	18.43	20.37	47.96

Fig. 13 shows that cities in south India (Bengaluru and Chennai) have maximum solar fraction at a collector slope of 0 º as they lie in the tropical region, and in the summer season, the solar radiations are directly falling in the tropics. The optimised parameters mentioned in Table 5 show that these two cities also have similar payback periods (PBP) and levelized cost of cooling (LCOC). The solar fraction (SF) is highest in New Delhi due to higher incident solar radiation, resulting in lower auxiliary heat energy consumption and reduced carbon dioxide emissions (CDE). The payback period (PBP) increasing in the order of New Delhi, Ahmedabad, Chennai, and Bengaluru is analogous to the decreasing incident solar radiation available in the cities. New Delhi exhibits better thermal, economic, and environmental performance, making it the most feasible and economically viable option among the cities (highest SF, lowest PBP, and lowest CDE) for the given parameters. The optimized parameters leading to a payback period (PBP) and levelized cost of cooling (LCOC) ranging from 18.43 to 21.93 years and 20.06 to 22.03 INR/kWh, respectively, exhibit resemblance to the numbers (19.7 years, 0.177$/kWh) determined by Sharma et al. (2023) for Jaipur city in India. The provision of subsidies on the investment cost for developing the solar absorption cooling system will further increase their potential for being developed in various cities and reduce the strain on the country's power grid. The natural gas fuel can be replaced with cheaper alternatives such as sugar cane bagasse, rice husk, or other biomass options to reduce the auxiliary fuel operating cost.

4. Conclusions

In this study, the thermal, economic, and environmental performance of a solar cooling system based on a vapour absorption system (VAS) using a solar compound parabolic collector (CPC) has been analysed for various climatic zones in India. A parametric study is carried out to understand the effect of solar collector area, storage tank specific volume ratio, and solar collector slope on solar fraction, collector useful energy gain, auxiliary heat energy consumption, payback period, levelized cost of cooling, and carbon dioxide emission. The system has been modelled in TRNSYS software. The conclusions of the work are mentioned below.

a) Collector area has a major impact on thermal, economic, and environmental analysis of solar absorption cooling systems.
b) The impact of the collector slope is confined to thermal analysis and demonstrated limited influence on economic and environmental aspects.
c) An increase in storage tank specific volume ratio (STSVR) for a fixed area does not significantly affect the solar fraction (SF). It affects economic and environmental analyses as auxiliary boiler energy consumption increases with increased storage tank volume.
d) The discounted payback period is higher than the simple payback period by 38% to 62% when the collector area varies from 100 m^2 to 1000 m^2 for the fixed value of collector slope and STSVR.
e) The parametric optimisation has been based on solar fraction for the collector slope and the discounted payback period for the solar collector area.

5. References

Al-Alili, A., Islam, M. D., Kubo, I., Hwang, Y., & Radermacher, R. (2012). Modeling of a solar powered absorption cycle for Abu Dhabi. Applied Energy, 93, 160–167.

Altun, A. F., & Kilic, M. (2020). Economic feasibility analysis with the parametric dynamic simulation of a single effect solar absorption cooling system for various climatic regions in Turkey. Renewable Energy, 152, 75–93.

Assilzadeh, F., Kalogirou, S. A., Ali, Y., & Sopian, K. (2005). Simulation and optimization of a LiBr solar absorption cooling system with evacuated tube collectors. Renewable Energy, 30(8), 1141–1159.

Balghouthi, M., Chahbani, M. H., & Guizani, A. (2012). Investigation of a solar cooling installation in Tunisia. Applied Energy, 98, 138–148.

Bellos, E., & Tzivanidis, C. (2017). Energetic and financial analysis of solar cooling systems with single effect absorption chiller in various climates. Applied Thermal Engineering, 126, 809–821.

Bhawan, S., & Puram, R. K. (2022). CO2 Baseline Database for the Indian Power Sector User Guide Government of India Ministry of Power Central Electricity Authority.

Eicker, U., & Pietruschka, D. (2009). Design and performance of solar powered absorption cooling systems in office buildings. Energy and Buildings, 41(1), 81–91.

Florides, G. A., Kalogirou, S. A., Tassou, S. A., & Wrobel, L. C. (2002). Modelling and simulation of an absorption solar cooling system for Cyprus. Solar Energy, Vol. 72, No. 1, pp. 43–51.

Gill, B., Saluja, S., & Palit, D. (2017). Electricity Pricing and the Willingness to Pay for Electricity in India: Current Understanding and the Way Forward. New Delhi: The Energy and Resources Institute (TERI).

Global Petrol Prices (2023). Global Petrol Prices. [WWW Document]. URL https://www.globalpetrolprices.com/ (accessed 08.01.2023)

Gogoi, T. K., & Saikia, S. (2019). Performance analysis of a solar heat driven organic Rankine cycle and absorption cooling system. Thermal Science and Engineering Progress, 13, 100372.

Hang, Y., Qu Ming, M., & Zhao, F. (2011). Economical and environmental assessment of an optimized solar cooling system for a medium-sized benchmark office building in Los Angeles, California. Renewable Energy, 36(2), 648–658.

Jha, I. S., Shri, Goyal, A., & Singh, P. K. (2022). Determination of levellised generic tariff for FY 2022-23 under Regulation 8 of the Central Electricity Regulatory Commission Regulations, 2020. Central Electricity Regulatory Commission, New Delhi.

Khan, M.S.A., Badar, A.W., Talha, T., Khan, M.W., & Butt, F.S. (2018) Configuration based modeling and performance analysis of single effect solar absorption cooling system in TRNSYS, Energy Conversion and Management, 157, 351e363.

Muye, J., Ayou, D. S., Saravanan, R., & Coronas, A. (2016). Performance study of a solar absorption power-cooling system. Applied Thermal Engineering, 97, 59–67.

Narayanan, M. (2017). Techno-economic analysis of solar absorption cooling for commercial buildings in India. International Journal of Renewable Energy Development, 6(3), 253–262.

Pranesh, V., Velraj, R., Christopher, S., & Kumaresan, V. (2019). A 50-year review of basic and applied research in compound parabolic concentrating solar thermal collector for domestic and industrial applications, Solar Energy, Volume 187, Pages 293-340.

Sharma, D. K., Sharma, D., & Ali, A. H. H. (2023). Optimization and thermo-economic performance of a solar-powered vapor absorption cooling system integrated with sensible thermal energy storage. Energy Conversion and Management: X, 20, 104400.

Sokhansefat, T., Mohammadi, D., Kasaeian, A., & Mahmoudi, A. R. (2017). Simulation and parametric study of a 5-ton solar absorption cooling system in Tehran. Energy Conversion and Management, 148, 339–351.

Utham, G., Agravat, S. M., Jani, B., & Bhutka, J. (2016). Modelling, Transient Simulation and Economic Analysis of Solar Thermal Based Air Conditioning System in Gujarat. Smart Grid and Renewable Energy, 07(08), 233–246.

Xu, Z. Y., & Wang, R. Z. (2017). Comparison of CPC driven solar absorption cooling systems with single, double, and variable effect absorption chillers. Solar Energy, 158, 511–519.